2022 I-RIM Conference
October 7-9, Rome, Italy
ISBN: 9788894580532
DOI:10.5281/zenodo.7531256

Considerations on possible approaches to measure risk for obstacle avoidance

Lorenzo Paiola
Centro di Ricerca "E. Piaggio"
DII Università di Pisa
Pisa, Italy
Istituto Italiano di Tecnologia
Genoa, Italy
lorenzo.paiola@iit.it

Giorgio Grioli
Centro di Ricerca "E. Piaggio"
Università di Pisa
Pisa, Italy
Istituto Italiano di Tecnologia
Genoa, Italy
giorgio.grioli@gmail.com

Antonio Bicchi
Centro di Ricerca "E. Piaggio"
Università di Pisa
Pisa, Italy
Istituto Italiano di Tecnologia
Genoa, Italy
antonio.bicchi@unipi.it

***Abstract*—Risk minimization has historically been tackled with chance constraints or with risk-aware measure acting on stochastic cost functions. To characterize risk in an obstacle avoidance setting, the computation of the probability of collision is of paramount importance.**

This paper explores and compares two approaches to compute such probabilities for a robot and an obstacle under Gaussian uncertainty along a continuous path. We first establish a theoretical framework, show numerical simulations, and finally we highlight the advantages and shortcomings of the considered approaches.

I. INTRODUCTION

Evaluating the *risk* associated to a set of action is becoming a question of paramount importance in the robotics field, as more and more autonomous systems are asked to perform safety-critical and human-centered tasks. Many applications including warehouse management, autonomous driving and cooperative robotics require the system not only to be *safe* in an instant in time, but to plan actions that also assure safety in the future. Uncertainty plays a central role in the process of associating a measure of how planned actions could be problematic: what the agent knows about itself and its environment can drastically change the evaluation of a possible plan.

The debate on what constitutes a *risk* entails various fields, from economics to the studies of dynamical systems [1] [2], but generally it is seen as the probability of an hazard weighted its severity. In robotics, risk minimization is traditionally associated to the field of stochastic optimization, where potentially all the variables involved in the optimization problem are random: while the control actions on the robot may be deterministic, the outcome of these actions will follow a possibly unknown probability density function. To account for such stochasticity in an optimization setting the usual tools are risk-aware measures [3] [4], which are mathematical operators that account for the tail of the probability density function of the cost, and chance constraints [5]–[8] that ensure that imposed restrictions on the states hold in a probabilistic sense. In the case of trajectory planning, the usual definition of risk is either *the probability of of the robot not being able to finish the path* [9], or *the probability of collision with an uncertain obstacle at any timestep* [5]. This paper explores two different ways of computing this probability in a continuous setting, what proprieties the two readings have and what additional features these fail to capture.

*This work was supported by the EU Project DARKO, Grant ID 101017274.

II. COLLISION EVENT

A. Background

Consider a robot and an obstacle living in a working environment $\mathbb{W} \subseteq \mathbb{R}^2$. Let $\mathbb{X}_R(x_R) \in \mathbb{W}$ be the set of points occupied by the robot and $\mathbb{X}_O(x_O) \in \mathbb{W}$ the set occupied by the obstacle, where $x_R \in \mathbb{W}$ and $x_O \in \mathbb{W}$ are the reference frames locations respectively of the robot and obstacle. The collision condition [6] is then defined as

$$C(x_R, x_O) : \mathbb{X}_R(x_R) \cap \mathbb{X}_O(x_O) \neq \{\emptyset\}. \tag{1}$$

The probability of this event is defined as

$$P(C) = \int_{x_R} \int_{x_O} I_C(x_R, x_O) p(x_R, x_O) dx_R dx_O, \tag{2}$$

where $I_C(x_R, x_O)$ is the indicator function of the set $\mathbb{X}_R(x_R) \cap \mathbb{X}_O(x_O)$ and $p(x_R, x_O)$ is the joint probability density function of x_R and x_O.

B. Problem Statement

Let's consider now the case where X_R and X_O are two i.i.d. Gaussian random variables (we capitalize these for clarity)

$$X_R \in \mathbb{W} \sim \mathcal{N}(\mu_R, \Sigma_R), \tag{3}$$

$$X_O \in \mathbb{W} \sim \mathcal{N}(\mu_O, \Sigma_O). \tag{4}$$

The distance between the robot and the obstacle $D_{RO} = X_R - X_O$ is an additional R.V. in $\mathbb{R}^2$ which follows the probability distribution

$$d_{RO}(x) = \mathcal{N}(x | \mu_R - \mu_O, \Sigma_T), \tag{5}$$

where $\Sigma_T = \Sigma_R + \Sigma_O$ is the combined covariance matrix [10].

The configuration space technique allows the problem of deterministic collision avoidance to be restated in terms of an emptied out set $\mathbb{X}_R$ and of an appropriately enlarged obstacle

set $\overline{\mathbb{X}}_O$ [11]. Following the same approach, but inverted in principle, we consider the obstacles to be punctual, and we enlarge the robot set $\overline{\mathbb{X}}_R$. We can then compute the probability of $D_{RO} \in \overline{\mathbb{X}}_R(0)$, the set occupied by the obstacle centered in the origin as

$$P(C) = \int_{\overline{\mathbb{X}}_R(0)} d_{RO}(x)dx. \tag{6}$$

This formula reframes the probability computation of the collision event from (2), removing the joint probability density function $p(x_R, x_O)$ from the calculation and integrating over a singular domain.

III. APPROACH

A. Event Definition

Computing the failure condition over a trajectory can lead to different results due to different definition of what constitutes a collision along a trajectory, the probability of which we define as *risk*.

The first way to interpret the collision event on the trajectory is to regard it to be a singular occurrence. Consider a unidimensional robot of thickness Δt moving along a path, orthogonal with respect to the robot's dimension, in $\mathbb{W}$. The area swept by such movement forms a tube, which we call $\mathbb{T}_R \in \mathbb{W}$, so that the collision condition becomes

$$C_{t0} : \mathbb{T}_R \cap \mathbb{X}_O \neq \{\emptyset\}. \tag{7}$$

The second possibility is to look at the robot moving along the path as multiple subsequent event. This prospective leads to a subdivision of the tube $\mathbb{T}_R$ along the direction of the trace as infinitesimal slices $\mathbb{T}_{Ri}$ of thickness Δt, so that $\mathbb{T}_{R1} \cup \mathbb{T}_{R2} \cup ... \cup \mathbb{T}_{Rn} = \mathbb{T}_R$ and $\mathbb{T}_{Ri} \neq \mathbb{T}_{Rj}\ \forall i \neq j$. The collision conditions are then

$$C_{ti} : \mathbb{T}_{Ri} \cap \mathbb{X}_O \neq \{\emptyset\}, \quad C_T : \bigvee_{i=1}^{n} C_{ti}. \tag{8}$$

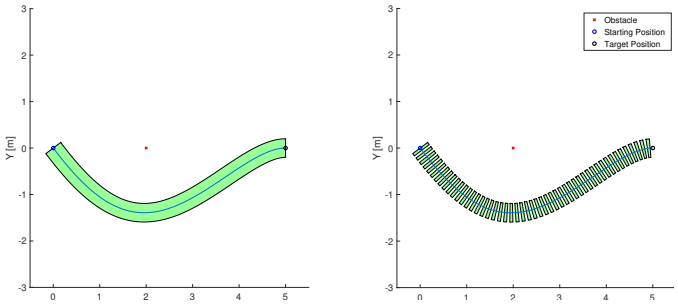

Fig. 1. Example of set $\mathbb{T}_R$ along with an approximate subdivision.

Assume now that

$$C_{ti} \perp C_{tj}\ \forall i \neq j, \tag{9}$$

then, using De Morgan's law, we can reformulate the collective condition of (8) as

$$C_T : \bigvee_{i=1}^{n} C_{ti} = \overline{\bigwedge_{i=1}^{n} \overline{C_{ti}}}. \tag{10}$$

The probability associated to (10) then is

$$P(C_T) = \lim_{n\to\infty} 1 - \prod_{i=1}^{n}(1 - P(C_{ti})). \tag{11}$$

These two approaches paint two faces of the same coin. In the first case the event is regarded as unique, and the stochastic variable associated with it has a singular realization: all the points inside $\mathbb{T}_R$ are considered at once. In the second procedure we're considering a stochastic process, as each event C_{ti} is its own i.i.d. random variable with an independent realization. Additionally, while the first interpretation considers time to be "frozen", the second method, studying a stochastic process, is compatible with its passage.

B. Tube parametrization and Probability Computation

Let the parametrization $\mu_R(s) : [0, 1] \to \mathbb{W}$ represent the path the robot will follow, with $s \in [0, 1]$ being the variable of the curvilinear parametrization. The tube $\mathbb{T}_R$ around such trace is parametrized with a function $\Phi(s, t) : [0, 1] \times \mathbb{R}_+ \to \mathbb{W}$ that in $\mathbb{R}^2$ can be built as a locally homeomorphic map

$$\Phi(s, \theta) = \begin{bmatrix} \mu_{Rx}(s) - \theta \frac{d\mu_{Ry}}{ds}(s) \\ \mu_{Ry}(s) + \theta \frac{d\mu_{Rx}}{ds}(s) \end{bmatrix}. \tag{12}$$

This allows us to compute the probability of collision for the whole tube $\mathbb{T}_R$ and a point-like obstacle as

$$P(C_{t0}) = \int_{-\Delta t}^{\Delta t} \int_0^1 \mathcal{N}(\Phi(\gamma, \theta)|\mu_O, \Sigma_T)|\det(\nabla\Phi)|d\gamma d\theta. \tag{13}$$

Remark: With (12) being only locally homeomorphic, and possibly parametrizing the same set in $\mathbb{W}$ multiple times, (13) will be only an approximation of (6), as we will discuss later. Considering now an infinitesimal partition along the path $\mu_R(s)$ of the tube $\mathbb{T}_R$, where the infinitesimal constituent is $ds \to 0$, the probability on the slice $\mathbb{T}_{Ri}$ can be computed as

$$P(C_{ti}) = \int_{-\Delta t}^{\Delta t} \mathcal{N}(\Phi(s_i, \theta)|\mu_O, C_T)\left|\left|\frac{d\mu_R}{d\gamma}\right|\right|d\theta ds. \tag{14}$$

The probability of $\bar{C}_T$ of no collision event happening is then the infinite product (11) of $(1 - P(C_{ti}))$ (14), and through the Volterra Product Integral [12] we rewrite it as

$$P(C_T) = 1 - \exp(-\int_0^1 \int_{-\Delta t}^{\Delta t} \mathcal{N}(\Phi(s, \theta)|\mu_O, \Sigma_T)\left|\left|\frac{d\mu_R}{ds}\right|\right|d\theta ds). \tag{15}$$

IV. NUMERICAL EXAMPLES

To show the behavior of the equations (13) and (15), some descriptive numerical examples are here displayed. Let us consider a simple case where (12) derives from the parametrized curve

$$\mu_1(s) = \begin{bmatrix} 5 - 2.5s \\ \cos(2\pi s) - 1 \end{bmatrix}, \tag{16}$$

with a fixed thickness $\Delta t = 0.1$. An obstacle is placed at $\begin{bmatrix} 3.75 & -0.05 \end{bmatrix}$ right before the starting position, as shown in figure 2. Σ_T is assigned to be the identity matrix multiplied by some scaling. Notice how (15) is always lower than (13)

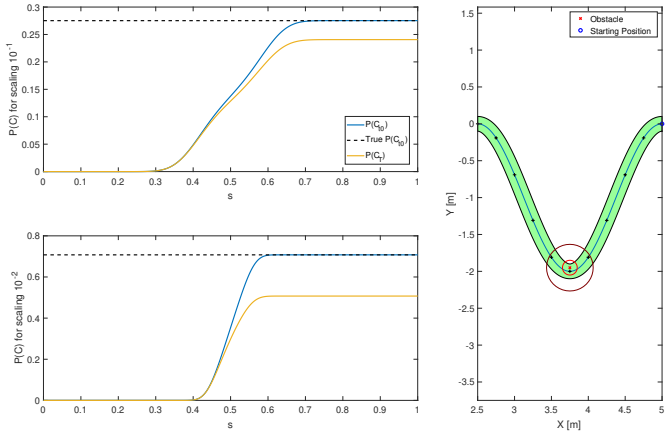

Fig. 2. Cosine path. Left: trend of (13) in blue and (15) in yellow. In black the true probability $P(C_T)$ obtained from (6) is highlighted. Right: (16) path parametrization with $\mathbb{T}_R$, black $+$ are placed at every 0.1 multiple in s. The circles the obstacle show a std of distance around the obstacle for the two covariances considered.

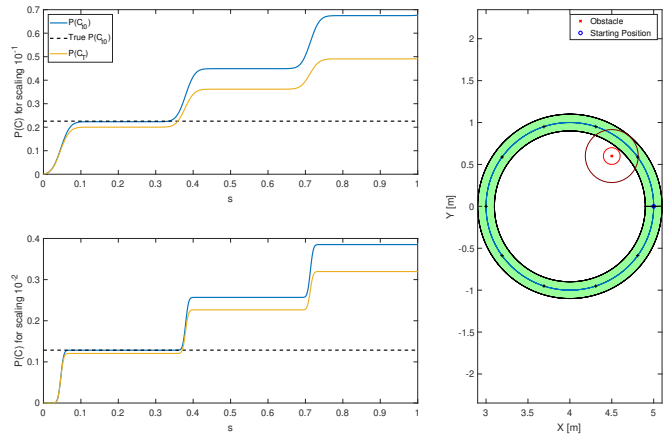

Fig. 3. Circular path with three turns.

while having the same trend. Also notice how at around $s \approx 0.5$, the nearest point to the obstacle, the slope of both the approaches changes. The growth in probability only happens around the obstacle at around $s \approx [0.3,\ 0.7]$, everywhere else the curves are stationary. While keeping the same thickness Δt, we consider a different parametrization of the path

$$\mu_2(s) = \begin{bmatrix} 4 + \cos(6\pi s) \\ \sin(6\pi s) \end{bmatrix}, \tag{17}$$

with an obstacle at $x_o = \begin{bmatrix} 4.5 & 0.6 \end{bmatrix}$. This path makes three turns around the circle, as shown in figure 17. At each full round the probability of collision stacks, in the case of (13) additively, while for (15) in a multiplicative way. Both figures 2 and 3 show the value of (6) on the set $\mathbb{T}_R$.

Consider now, instead, the case in which Δt is variable inside the range $[0, 1.2]$, and the covariance matrix $\Sigma_T = I$ is fixed with scaling 10^{-1} and 10^{-2}. The trace under scrutiny is

TABLE I
COMPARISON BETWEEN THE VALUES OBTAINED FROM (13) AND (6) IN BOTH SCENARIOS SHOWN IN FIGURE 2 AND 3.

Path\Scaling	(13) $P(C_T)$, $s=1$	(6) True $P(C_T)$, $s=1$	$P(C_T)$, $s=\frac{1}{3}$
Cosine\$10^{-1}$	0.275253	0.275188	/
Cosine\$10^{-2}$	0.707647	0.707559	/
Circle\$10^{-1}$	0.677078	0.225779	0.223350
Circle\$10^{-2}$	0.385130	0.129458	0.128376

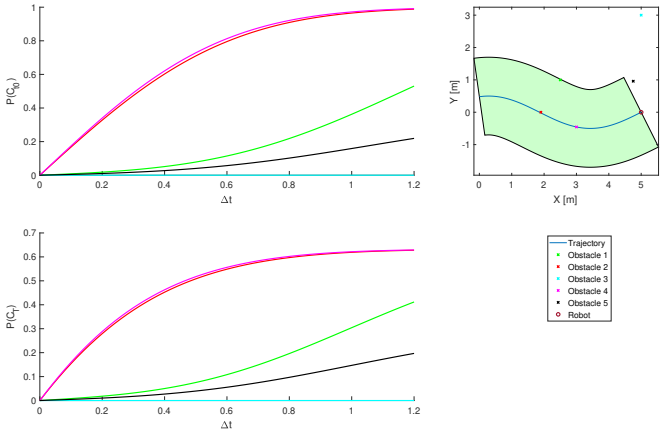

Fig. 4. Scaling at 10^{-1} Left: trend of (13) and (15) against Δt, multiple obstacle considered. Right: (18) path parametrization with largest $\mathbb{T}_R$.

the one of figure 4 parametrized by

$$\mu_3(s) = \begin{bmatrix} 5(1-s) \\ 0.5\sin(5s) \end{bmatrix}, \tag{18}$$

where the probabilities (13) and (15) are computed on the whole trajectory.

We see how the probabilities computed are very dependent on the scaling considered, with scaling 10^{-2} the slope of the graphs is very steep and obstacles that aren't near the path aren't influential on the computation. Also notice how (13) covers the whole range $[0, 1]$ of possible probabilities, while (15) caps at $1 - e^{-1}$.

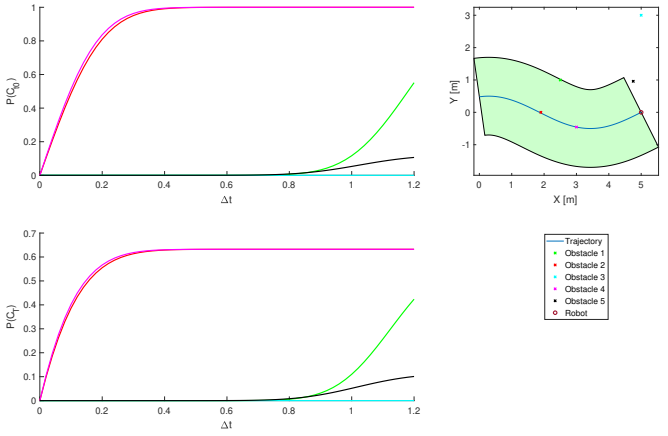

Fig. 5. Scaling at 10^{-2} Left: trend of (13) and (15) against Δt, multiple obstacle considered. Right: (18) path parametrization with largest $\mathbb{T}_R$.

TABLE II
OBSTACLE POSITION IN FIGURE 4, 5.

Obstacle	1	2	3	4	5
Position	$\begin{bmatrix}2.5\\1\end{bmatrix}$	$\begin{bmatrix}1.9\\0\end{bmatrix}$	$\begin{bmatrix}5\\3\end{bmatrix}$	$\begin{bmatrix}3\\-0.455\end{bmatrix}$	$\begin{bmatrix}4.76\\0.96\end{bmatrix}$

V. DISCUSSION

The method considered shows promise, as, thanks to the continuous approach to the parametrization, it characterizes the probability of collision without the need of subdividing the trace in "stages" using Boole's Lemma [6] [13]. The continuous nature of the two approaches makes the measure more robust with respect to methods based e.g. on occupancy grids [9]. Indeed, in such methods, the computed risk depends on the discretization of the grid, which is an issue that doesn't appear in our approach.

The same continuous nature also brings disadvantages, the main one being the double integral present both in (13) and (15), which makes the approaches computationally inefficient.

The behavior of periodic and overlapping paths, shown in figure 3, is also worthy of discussion. The first thing to notice is how the probability of collision defined by (13) adds onto itself at each revolution, while (15) is multiplicative following (11) (e.g. with three turns $P(C_T) = 1 - (1 - P(C_t))^3$, where $P(C_t)$ is the value of (15) after a revolution). Evidently the additivity of (13) is an issue, in fact if the path is repeated too many times, the probability $P(C_{t0})$ may result in a value greater than 1. So while this approximation of (6) seems sound, as also shown in table I, the computation of the probability of recurring traces can lead to non-sensical results without additional considerations or alternative approaches to define the integration set. The multiplicativity of (15), instead, not only ensures that $P(C_T) \in [0, 1]$ for repeated trajectories, but also lets us consider subsets of the path $\mu(s)$ as independent and decompose the probability as

$$P(\bar{C}_T, s_0, s_f) = P(\bar{C}_T, s_0, s^*)P(\bar{C}_T, s^*, s_f), \qquad (19)$$

$\forall s_0 \leq s^* \leq s_f \in [0, 1]$. This probability decomposition can be interpreted as the "risk to go": the path traversed between s_0 and s^* doesn't influence the risk computation on the remaining part of the path.

Other issues appear, for both approaches, around the choice of Δt. The first concern is a conceptual one, as we'd like to have a measure of *risk* which is intrinsic to the path and the environment, not based on a parameter dependent on the dimensions of the robot. The second point is that by considering a too large Δt the probability computations are not valid anymore. This happens because (12) is only locally homeomorphic, so that in the case of (15) the sets $\mathbb{T}_{Ri}$ overlap and (9) doesn't hold anymore, while for (13) the set $\mathbb{T}_R$ folds onto itself leading to inaccurate results. This is what happened in figure 2, where a single obstacle has been accounted for twice and a change of slope appears, and what would have happened in figure 3 if Δt had become large enough.

VI. CONCLUSIONS

We have presented two methods of computing the probability of collision between a robot and an obstacle under Gaussian uncertainty. We've formally reasoned about the definition of collision event and how different interpretations of it lead to different formulations of its probability. The expressions found have then been compared through some numerical examples and both boons and disadvantages have been discussed.

In future work we plan to work on these disadvantages, particularly we would like to make the measure of *risk* intrinsic to the parametrization and not dependent on the robot's size.

REFERENCES

[1] G. A. Holton, "Defining Risk," *Financial Analysts Journal*, vol. 60, no. 6, pp. 19–25, Nov. 2004.

[2] P. Whittle, "RISK SENSITIVITY, A STRANGELY PERVASIVE CONCEPT," *Macroecon. Dynam.*, vol. 6, no. 1, pp. 5–18, Feb. 2002.

[3] A. Majumdar and M. Pavone, "How Should a Robot Assess Risk? Towards an Axiomatic Theory of Risk in Robotics," in *Robotics Research*, N. M. Amato, G. Hager, S. Thomas, and M. Torres-Torriti, Eds. Cham: Springer International Publishing, 2020, vol. 10, pp. 75–84.

[4] F. Farshidian and J. Buchli, "Risk Sensitive, Nonlinear Optimal Control: Iterative Linear Exponential-Quadratic Optimal Control with Gaussian Noise," *arXiv:1512.07173 [cs]*, Dec. 2015.

[5] W. Han, A. Jasour, and B. Williams, "Non-Gaussian Risk Bounded Trajectory Optimization for Stochastic Nonlinear Systems in Uncertain Environments," Mar. 2022.

[6] N. E. Du Toit and J. W. Burdick, "Probabilistic Collision Checking With Chance Constraints," *IEEE Trans. Robot.*, vol. 27, no. 4, pp. 809–815, Aug. 2011.

[7] L. Blackmore and M. Ono, "Convex Chance Constrained Predictive Control Without Sampling," in *AIAA Guidance, Navigation, and Control Conference*. Chicago, Illinois: American Institute of Aeronautics and Astronautics, Aug. 2009.

[8] A. Shapiro, D. Dentcheva, and A. Ruszczyński, *Lectures on Stochastic Programming: Modeling and Theory*. Society for Industrial and Applied Mathematics, Jan. 2009.

[9] X. Xiao, J. Dufek, and R. R. Murphy, "Robot Risk-Awareness by Formal Risk Reasoning and Planning," *IEEE Robot. Autom. Lett.*, vol. 5, no. 2, pp. 2856–2863, Apr. 2020.

[10] A. Tarantola, *Inverse Problem Theory and Methods for Model Parameter Estimation*. Society for Industrial and Applied Mathematics, Jan. 2005.

[11] S. M. LaValle, *Planning Algorithms*. Cambridge: Cambridge University Press, 2006.

[12] A. Slavík, *Product Integration, Its History and Applications*, ser. History of Mathematics. Praha: Matfyzpress, 2007, no. 29.

[13] S. Patil, J. van den Berg, and R. Alterovitz, "Estimating probability of collision for safe motion planning under Gaussian motion and sensing uncertainty," in *2012 IEEE International Conference on Robotics and Automation*. St Paul, MN, USA: IEEE, May 2012, pp. 3238–3244.